Online Sequential Compressed Sensing with Weighted Multiple Side Information for Through the Wall Imaging

Becquaert, Mathias ; Cristofani, Edison; Vandewal, Marijke; Stiens, Johan; Deligiannis, Nikolaos

Published in:
URSI Benelux Forum 2018

Publication date:
2018

Document Version:
Accepted author manuscript

Online Sequential Compressed Sensing with Weighted Multiple Side Information for Through the Wall Imaging

Mathias Becquaert[1,2], Edison Cristofani[1,2], Marijke Vandewal[1], Johan Stiens[2], and Nikos Deligiannis[2]

[1]CISS Department, Royal Military Academy, 30 Av. de la Renaissance, B-1000 Brussels
[2]ETRO Department, Vrije Universiteit Brussel, Pleinlaan 2, B-1050 Brussels, Belgium

***Abstract*—In this paper we propose a new approach for applying Compressed Sensing to Stepped Frequency Continuous Wave SAR measurements. The proposed technique allows the sensor to decide autonomously, while scanning, on the number of samples needed, while assuring a reconstruction quality chosen by the operator. With the online reconstruction algorithm sampling rates far below the bound fixed by the Nyquist-Shannon theorem are achieved. Moreover, to improve further on minimizing the frequency sampling rates, the measurements obtained from previous sensor positions are added as online weighted side information into the reconstruction algorithm. The applicability and excellent performance of the approach is illustrated by a series of experiments on sparsified Through-the-Wall Imaging radar data.**

I. Introduction

Over the past decade, Compressed Sensing (CS) has been introduced into a large variety of applications confronted with large data volumes, long measurement times, gapped data or expensive hardware, such as: medical imaging [1], radar imaging [2], spectroscopy [3] and telecommunications [4].
Through-the-Wall Imaging (TWI) radars are emitting wide-band signals and using large (synthetic) antenna apertures in order to deliver high resolution images. CS has been proven to offer an effective solution to reduce the number of samples needed to obtain high-resolution images [5], [6], [7]. This new CS sub-Nyquist sampling bound is function of the sparsity or compressibility of the radar image. Through-the -Wall radar data are a hard candidate for CS, since they are polluted with undesired effects, originating from the interaction between the sensing waves and the walls, such as wall ringing, ghost targets and wall-clutter. Lot of effort has gone in suppressing these effects and thereby sparsifying the radar images, for example: spatial filtering [8], singular value decomposition [9] or multipath exploitation [10].

II. Contributions

(1) Previous work on CS applied to TWI radars, published in literature, concentrates on further lowering the subsampling bound and thereby minimizing the required number of samples in range or cross-range direction. These sampling bounds are function of the sparsity or compressibility of the radar image, which implies that the radar operator needs to know or guess the sparsity of the radar image, prior to the measurement, in order to be able to obtain the image from a minimum number of samples. The work in this paper leverages this chicken-or-egg problem by using a sequential reconstruction approach allowing to determine an upper bound for the reconstruction error. In other words, the operator needs now to decide on the desired reconstruction quality instead of guessing the sparsity of the unknown image.

(2) The online algorithm proposed in this work reconstructs the subsampled signal in range direction taking advantage of the similarity between the signal at the current scanning position and the signals obtained from previous SAR positions. Indeed, if the sensor moves parallel to the wall, the contributions in the signal due to the presence of the wall, can be assumed to show a high degree of similarity over the different scanning positions. This similarity is exploited by adding the previous reconstructed range signals as weighted Side Information (SI) into the CS minimization equation.

III. Background

A. Compressed Sensing

Suppose $x \in \mathbb{C}^N$ to be the unknown vector which needs to be reconstructed. To do so, x is sensed by applying the sensing matrix $A \in \mathbb{C}^{n \times N}$, resulting in n linear measurements:

$$y = Ax. \tag{1}$$

The solution, $\hat{x}$, of this set of equations is unique only if $n = N$.

CS theory states [11] [12] that x can be reconstructed correctly, under certain conditions [13] [14], with high probability when $n << N$ if x happens to be sparse, i.e. x has k non-zero elements (with $k << N$), by solving the following minimization problem:

$$min \, \|x\|_{l0} \quad \text{s.t.} \quad \|Ax - y\|_{l2} \leq \epsilon, \tag{2}$$

which can be relaxed to the convex optimization problem:

$$min \, \|x\|_{l1} \quad \text{s.t.} \quad \|Ax - y\|_{l2} \leq \epsilon. \tag{3}$$

Suppose that the sparsity of x is not the only prior knowledge available and suppose z to be a vector sharing a high degree of similarity with x. This extra prior knowledge can be added as SI to the minimization equation [15]:

$$\min_x \{\frac{1}{2}\|Ax-y\|_{l2}^2 + \lambda(\|x\|_{l1} + \|x-z\|_{l1})\}. \quad (4)$$

Which can be extrapolated to a weighted n-$l1$ problem with J SIs z_j [16] :

$$\min_x \{\frac{1}{2}\|Ax-y\|_{l2}^2 + \lambda \sum_{j=0}^{J} \beta_j(\|W_j(x-z_j)\|_{l1})\}, \quad (5)$$

with inter-SI weights β_j between the J SIs and $W_j = diag(w_{j1}, w_{j2}, ..., w_{jn})$ with w_{ij} the inter-SI weights.

B. Sequential Compressed Sensing

Suppose $\hat{x}^M$ to be the CS reconstruction of the vector x after taking M linear measurements. We will now establish a strategy to estimate a bound for the reconstruction error

$$\delta = \hat{x}^M - x, \quad (6)$$

by adding a few (T) new samples: y_i with $1 \leq i \leq T$ to the existing set of M samples [17].
For each new sample, a deviation error z_i:

$$z_i = \hat{y}_i - y_i, \quad (7)$$

can be calculated between the actual true sample y_i and an estimation $\hat{y}_i$ of the sample obtained by performing a synthetic measurement of $\hat{x}^M$:

$$\hat{y}_i = A(i,:)\hat{x}^M. \quad (8)$$

The deviation errors can thus be expressed as:

$$z_i = A(i,:)\delta, \quad 1 \leq i \leq T \quad (9)$$

and are i.i.d. from a distribution with a variance equal to $\|\delta\|_2^2 Var(A(i,j))$ [17] . If $Var(A(i,j)) = 1$, then $\|\delta\|_2^2$ can be obtained through estimating the variance of the T deviation errors. Define:

$$Z_T \triangleq \frac{\sum_T z_i^2}{\|\delta\|_2^2}, \quad (10)$$

which is a χ^2 random variable with T degrees of freedom. For a small value α, the largest z^* can be obtained through the χ_T^2 cumulative function such that $p(Z_T \leq z^*) \leq \alpha$. This means that δ is bounded by $\sqrt{\frac{\sum_T z_i^2}{z^*}}$ with a probability of $1-\alpha$.

C. Through-the-Wall Radar Imaging

The TWI sensor used for the experiments is a Stepped-Frequency Continuous Wave (SFCW) SAR emitting L discrete frequencies:

$$s(t) = \sum_{l=1}^{L} \text{rect}\left(\frac{t-lT_p}{T_p}\right)\exp(j2\pi f_l t), \quad (11)$$

Where rect(.) is the rectangular function and T_p the complete period to emit the whole bandwidth.

This signal is received after reflection on K point targets at t equal to the Round Trip Time (RTT). Which, after homodyne demodulation, results in a beat signal:

$$s_b = \sum_{k=1}^{K}\sum_{l=1}^{L} a_{k,l}\exp\Big(-j2\pi f_l.RTT\Big). \quad (12)$$

IV. Experiments

A. Simulations

The applicability of sequential CS for radar measurements is illustrated through simulations for two types of measurements:
(1) The reconstruction of a range profile: for this type of measurements, y corresponds to the signal received at a single sensor position and the sensing matrix A is a Discrete Fourier (DFT) matrix.
(2) The reconstruction of a radar SAR image: In this case y corresponds to a complete SAR measurement and each column of the matrix A is populated by the vectorized beat signals (12) coming from a single target of dimensions equal to the resolution cell at one specific pixel location. The number of columns of A is thus equal to the number of pixels in the radar image.

Two random sparse vectors x_1 and x_2 of length N = 400 are created, with k = 4 and k = 20 non-zero elements respectively. During the first iteration, the vectors x_1 and x_2 are reconstructed: $\hat{x}_1$ and $\hat{x}_2$, with only 2% of samples, randomly selected. At each iteration 2% of samples are added to the set of selected samples, the true reconstruction error δ is measured and the bound for δ is calculated with a probability $1-\alpha$ = 0.99.
The results of this experiment are depicted in Fig. 1. The upper graph shows the results for the reconstruction using a DFT matrix as sensing matrix (A), while the lower graph depicts the results for A = SAR sensing matrix. In both cases and for both k = 4 (blue graphs) and k = 20 (red graphs), the true error δ (full line) is closely and correctly bounded by the estimated error bound (dashed line).

B. Through the Wall Imaging data

(1) TWI Measurement:

Real TWI data was obtained through a TWI radar prototype, consisting of a Vector Network Analyzer (Rhod&Schwarz, ZVA24) connected to a single Antenna (Schwarzbeck BBHA9120D) and placed on a motorized platform. The platform was moving on a rail placed parallel to the wall and taking $S11$-measurements adhering to a stop an go method.

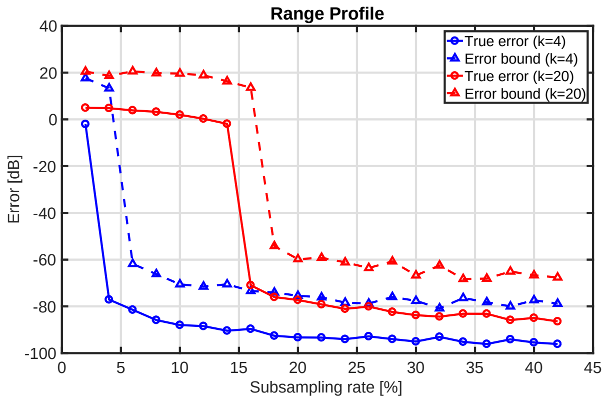

(a)

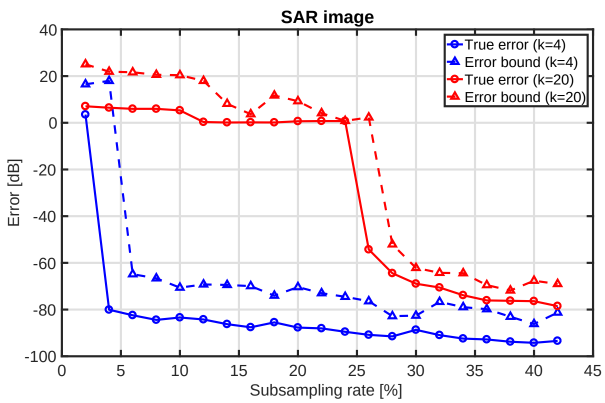

(b)

Fig. 1. True errors (full curve) and estimated error bounds (dashed curves) for increasing sampling rates. (a) A is a DFT matrix and (b) A is a SAR sensing matrix.

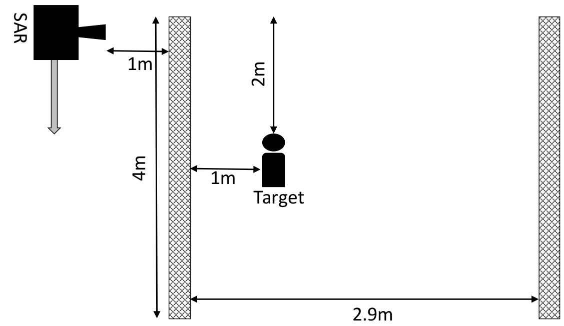

(a)

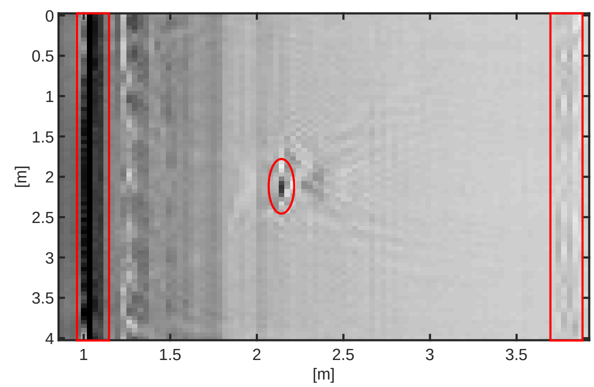

(b)

Fig. 2. (a) Geometric setup of the through-the-wall radar measurement. With, from left to right: the SAR radar, the first wall, a human target and the second wall. (b) Range Doppler processed TWI measurement with the walls framed in red and the target encirceld in red.

TABLE I
SPECIFICATIONS OF THE SENSOR USED FOR THE EXPERIMENTS

Sensor parameters	**Value**
Starting frequency f_0	1 GHz
Bandwidth	4 GHz
Frequency step Δf	10 MHz
Scanning distance	4 m
Number of azimuth measurements	80
Number of frequencies	94
Aperture angle (-3 dB) at 3 GHz	40°
Range resolution	0.038 m
Cross-range resolution	0.07 m

The specifications of the used prototype are listed in table I.

The scene consisted of two parallel walls, built from piled aerated concrete blocks (thickness = 0.15m) delimiting a room of 4m (in cross-range direction) by 2.9m (in range direction). Inside the room a human target was placed 1m behind the first wall and at a distance of 2m in cross-range distance. A schematic representation of the setup is shown in Fig. 2, together with the image obtained by applying a Range Doppler algorithm on the measurement. The data used in the remainder of this paper is the TWI data obtained through this expermiment which was then sparsified by synthetically lowering the measurement noise in the data by 10dB.

(2) Online Sequential Compressed Sensing:

Sequential CS allows to reconstruct a signal by sequentially adding samples until a chosen reconstruction quality can be guaranteed with high probability. The authors of this paper chose to use the sequential CS strategy to reconstruct the range profile at each sensor position subsequently, instead of reconstructing the SAR image as a whole, for three reasons: (a) This choice allows an adaptive subsampling rate. At each position a different sampling rate can be chosen, tailored to the sparsity of the portion of the scene, sensed from this position. If the sensor faces an almost empty zone, the number of samples will automatically be lowered. (b) The information obtained through the measurements at previous scanning positions can be added as Side Information (SI) if an online algorithm is used for reconstructing the range profile at a sensor position, before moving to the next scanning position. (c) Using a sequential CS approach for the reconstruction of the SAR image at once, would imply that at each iteration a new scan of the scene needs to be performed, which would make this option very time consuming (a single scan over 4m with the radar described in this paper takes 6min58sec).

The diagrams depicted in Fig. 3 show the values of true

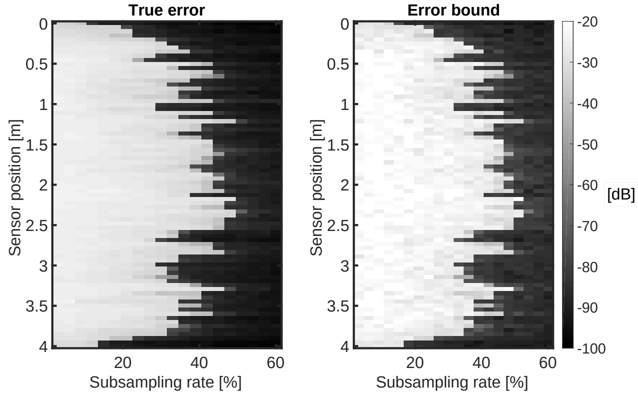

Fig. 3. True error and estimated error bounds over the different scanning positions and for increasing sampling rates.

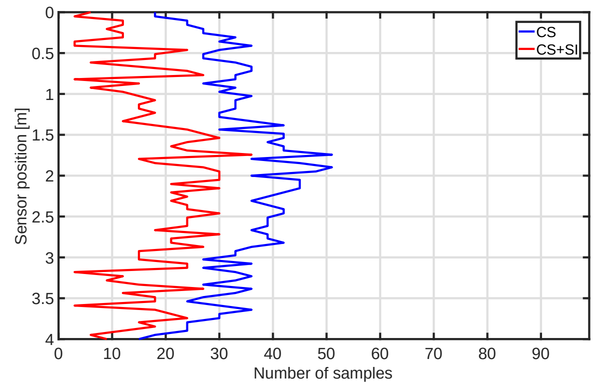

Fig. 4. Number of Samples, over the different scanning positions, required to satisfy a maximum reconstruction error of -35dB by applying CS with (red curve) and without (blue curve) weighted SI.

errors (on the left-hand side) and the estimated bounds (on the right-hand side) for the reconstruction of the range profile for each scanning position (vertical axis) and for sequentially adding new samples with a step size of 3 samples (horizontal axis). The estimated error bounds perfectly the true error, and is thus an excellent candidate to serve as stopping critirion for interrupting the iterative addition of samples.

(3) Adding Side Information:

The obtained subsampling rates can further be lowered. The severe contributions of a wall parallel to the scanning path can be considered to be almost constant over the different scanning positions. This implies that the different range profiles along the sensor positions show a high degree of similarity amongst them. Besides the assumed sparsity of the range profile, the range profiles form previous sensor positions can be added as weighted SIs, allowing a correct reconstruction from even less samples by solving the minimization problem (5). The work in [16] proposes an algorithm for solving this minimization problem, computing adaptive weights inter and intra the SIs, taking into account the different qualities of SIs.

Fig. 4 depicts the required portion of samples (horizontal axis), out of 99 samples, needed to ensure an arbitrary chosen reconstruction error of -35dB over the different sensor positions (vertical axis) through reconstruction without (blue curve) and with (red curve) weighted SI. A mean subsampling rate of 18% suffices to fulfill the desired reconstruction quality request with a probability equal to 0.99. Fig. 5 shows the corresponding obtained range profiles, before cross-range compression (lower graph), compared to the reconstructed range profiles from the fully sampled data (upper graph).

V. Conclusions and Future Work

The practical and useful implementation of compressed sensing in SAR measurements faces a fundamental problem: ”how can the operator determine the number of samples needed to reconstruct a radar image with unknown sparsity?” In this paper, we demonstrated that sequential CS leverages this problem and allows an automatic decision of the number

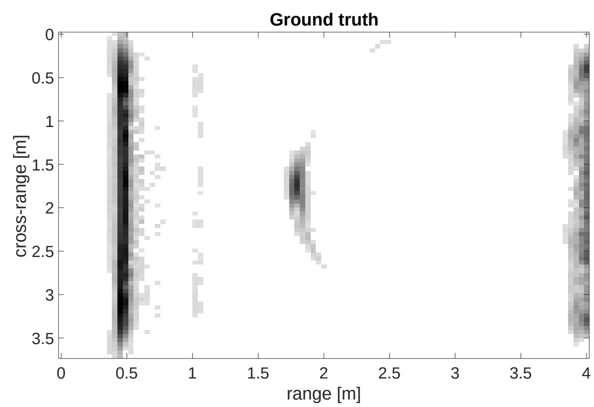

(a)

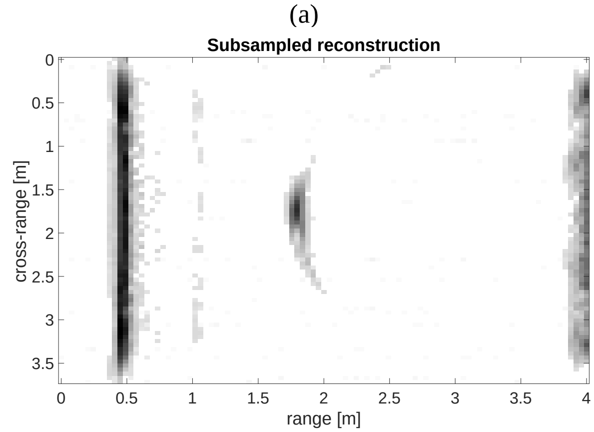

(b)

Fig. 5. (a) Reconstructed range profiles with 100% of the samples. (b) Reconstructed range profiles with a mean subsampling rate of 18%, distributed over the different scanning positions as depicted in Fig. 4.

samples based the operators choice of reconstruction quality. The sequential CS approach was implemented online, reconstructing range profiles while the TWI sensor was moving along the wall and meanwhile expanding his prior knowledge with the profiles obtained from previous scanning positions. The proposed solution allows a severe subsampling and autonomously adapts the sampling rate along the scanning path in order to achieve a desired reconstruction quality.

Future work will concentrate on applying this technique on noisy data and near sparse data, by adding the stochastic properties of the noise in the estimation of the error bound.

REFERENCES

[1] M. Lustig, D. Donoho, and J. M. Pauly, "Sparse mri: The application of compressed sensing for rapid mr imaging," *Magnetic resonance in medicine*, vol. 58, no. 6, pp. 1182–1195, 2007.

[2] R. Baraniuk and P. Steeghs, "Compressive radar imaging," in *Radar Conference, 2007 IEEE*. IEEE, 2007, pp. 128–133.

[3] K. Kazimierczuk and V. Y. Orekhov, "Accelerated nmr spectroscopy by using compressed sensing," *Angewandte Chemie International Edition*, vol. 50, no. 24, pp. 5556–5559, 2011.

[4] Z. Tian and G. B. Giannakis, "Compressed sensing for wideband cognitive radios," in *Acoustics, Speech and Signal Processing, 2007. ICASSP 2007. IEEE International Conference on*, vol. 4. IEEE, 2007, pp. IV–1357.

[5] Y.-S. Yoon and M. G. Amin, "Through-the-wall radar imaging using compressive sensing along temporal frequency domain," in *Acoustics Speech and Signal Processing (ICASSP), 2010 IEEE International Conference on*. IEEE, 2010, pp. 2806–2809.

[6] M. Leigsnering, C. Debes, and A. M. Zoubir, "Compressive sensing in through-the-wall radar imaging," in *Acoustics, Speech and Signal Processing (ICASSP), 2011 IEEE International Conference on*. IEEE, 2011, pp. 4008–4011.

[7] Q. Huang, L. Qu, B. Wu, and G. Fang, "Uwb through-wall imaging based on compressive sensing," *IEEE Transactions on Geoscience and Remote Sensing*, vol. 48, no. 3, pp. 1408–1415, 2010.

[8] Y.-S. Yoon and M. G. Amin, "Spatial filtering for wall-clutter mitigation in through-the-wall radar imaging," *IEEE Transactions on Geoscience and Remote Sensing*, vol. 47, no. 9, pp. 3192–3208, 2009.

[9] R. Chandra, A. N. Gaikwad, D. Singh, and M. Nigam, "An approach to remove the clutter and detect the target for ultra-wideband through-wall imaging," *Journal of Geophysics and Engineering*, vol. 5, no. 4, p. 412, 2008.

[10] M. Leigsnering, F. Ahmad, M. Amin, and A. Zoubir, "Multipath exploitation in through-the-wall radar imaging using sparse reconstruction," *IEEE Transactions on Aerospace and Electronic Systems*, vol. 50, no. 2, pp. 920–939, 2014.

[11] D. L. Donoho, "Compressed sensing," *IEEE Transactions on information theory*, vol. 52, no. 4, pp. 1289–1306, 2006.

[12] E. J. Candès, J. Romberg, and T. Tao, "Robust uncertainty principles: Exact signal reconstruction from highly incomplete frequency information," *IEEE Transactions on information theory*, vol. 52, no. 2, pp. 489–509, 2006.

[13] E. J. Candes, "The restricted isometry property and its implications for compressed sensing," *Comptes Rendus Mathematique*, vol. 346, no. 9-10, pp. 589–592, 2008.

[14] A. M. Tillmann and M. E. Pfetsch, "The computational complexity of the restricted isometry property, the nullspace property, and related concepts in compressed sensing," *IEEE Transactions on Information Theory*, vol. 60, no. 2, pp. 1248–1259, 2014.

[15] J. F. Mota, N. Deligiannis, and M. R. Rodrigues, "Compressed sensing with side information: Geometrical interpretation and performance bounds," in *Signal and Information Processing (GlobalSIP), 2014 IEEE Global Conference on*. IEEE, 2014, pp. 512–516.

[16] H. Van Luong, J. Seiler, A. Kaup, and S. Forchhammer, "A reconstruction algorithm with multiple side information for distributed compression of sparse sources," in *Data Compression Conference (DCC), 2016*. IEEE, 2016, pp. 201–210.

[17] D. M. Malioutov, S. R. Sanghavi, and A. S. Willsky, "Sequential compressed sensing," *IEEE Journal of Selected Topics in Signal Processing*, vol. 4, no. 2, pp. 435–444, 2010.